Generic Contrast Agents
Our portfolio is growing to serve you better. Now you have a *choice*.
FRESENIUS KABI
VIEW CATALOG

AJNR

Reduction of Radiation Dose for Cerebral Angiography Using Flat Panel Detector of Direct Conversion Type: A Vascular Phantom Study

Y. Hatakeyama, S. Kakeda, N. Ohnari, J. Moriya, N. Oda, K. Nishino, W. Miyamoto and Y. Korogi

This information is current as of May 9, 2025.

AJNR Am J Neuroradiol 2007, 28 (4) 645-650
http://www.ajnr.org/content/28/4/645

ORIGINAL RESEARCH

Reduction of Radiation Dose for Cerebral Angiography Using Flat Panel Detector of Direct Conversion Type: A Vascular Phantom Study

Y. Hatakeyama
S. Kakeda
N. Ohnari
J. Moriya
N. Oda
K. Nishino
W. Miyamoto
Y. Korogi

BACKGROUND AND PURPOSE: Compared with image intensifier television (I.I.-TV) system, an angiography system using the flat panel detector (FPD) of direct conversion type has a high spatial resolution, which may improve image quality, reduce patient exposure, or both. Our purpose was to evaluate the detection of simulated aneurysmal blebs under dose reduction with the FPD system in comparison with the I.I.-TV system.

MATERIALS AND METHODS: A vascular phantom was designed to simulate various intracranial aneurysms with and without blebs, and this phantom was filled with 3 different concentrations of contrast material (300, 150, and 100 mg I/mL). 2D digital subtraction angiography (DSA) at low-dose mode of FPD system was compared with 2D DSA at a standard-dose mode of FPD system and a conventional mode of I.I.-TV system. Data analysis was based on 171 observations (57 aneurysms [20 with bleb and 37 without bleb] × 3 contrast material concentrations) by each of 7 radiologists, and the detection performances of blebs were compared using a receiver operating characteristic (ROC) analysis.

RESULTS: The mean dose measurements with a phantom during 2D DSA were 0.36 mGy/frame with low-dose mode of FPD system, 0.72 mGy/frame with standard-dose mode of FPD system and 0.76 mGy/frame with I.I.-TV system. The mean Az at 100 mg I/mL was significantly higher for low-dose mode of FPD than for conventional-dose mode of I.I.-TV mean Az, 0.85 versus 0.56; $P < .01$), though differences were not significant with 150 and 300 mg I/mL between both systems.

CONCLUSION: The FPD system allows a considerable dose reduction during 2D DSA without loss of the image quality.

Interventional neuroradiologic procedures may cause large doses of radiation to be delivered to the craniofacial region.[1,2] In recent years, because of the increasing number of procedures performed and the lengthy exposures involved, there has been a growing concern regarding the detrimental effects (examples of deterministic effects are early transient erythema and hair loss) of radiation to patients during guided interventional procedures. In fact, radiation-induced patient skin injuries have been reported to result from extended exposures in interventional procedures. Kuwayama et al[3] have reported transient alopecia in 2 patients who underwent endovascular neurologic interventions; in each patient, the measured dose at the temporal area was approximately 4.2 Gy. Moreover, diagnostic and interventional radiologic procedures in the head, in particular those involving the orbits, inevitably carry a risk of radiation exposure to the lens of the eye.[4,5]

Results of various studies in plain radiography have already revealed that the direct read-out flat panel detector (FPD) systems yield superior image quality and have a lower radiation dose requirement as compared with screen-film systems.[6-10] However, no studies have evaluated digital subtraction angiography (DSA) obtained by the angiography system using the FPD. An angiography system using the FPD of direct conversion type, in which amorphous selenium (a-SE) is used as the conversion layer, has become commercially available. Compared with an image intensifier television (I.I.-TV) system, this angiography system using the FPD has several theoretic advantages, such as high spatial resolution, wide dynamic range, square field-of-view, and real-time imaging capabilities with no geometric distortion, which may be used for improved image quality, reduced patient exposure, or both. In this study, we compared 2D DSA on an FPD system with a conventional I.I.-TV system for the detection of simulated aneurysmal blebs using observer performance study and sought to examine the potential for dose reduction of 2D DSA with an angiography system using the FPD.

Received April 22, 2006; accepted after revision June 26.

From the Department of Radiology (Y.H., S.K., N.O., J.M., N.O., Y.K.), University of Occupational and Environmental Health School of Medicine, Kitakyushu, Japan; and Medical Systems Division (K.N., W.M.), Shimadzu Corporation, Japan.

Address correspondence to Shingo Kakeda, MD; Department of Radiology, University of Occupational and Environmental Health, 1-1 Iseigaoka, Yahatanishi-ku, Kitakyushu 807-8555, Japan; e-mail: kakeda@med.uoeh-u.ac.jp

Materials and Methods

Specification of I.I.-TV and FPD System

The main technical features of the 2 systems are summarized in Table 1. The I.I. TV-system consisted of a 0.6-mm focal spot and a 10-inch (254-mm) cesium iodide image-intensifying tube (KXO-80C/D and DFP-2000A; Toshiba Medical Systems, Tokyo, Japan) that had been in routine use for about 1 year. The FPD angiography system consisted of a FPD of direct conversion type on a motorized C-arm (Safire; Shimadzu Corporation, Kyoto, Japan). This newly developed detector has a pixel pitch of 150 μm, covering a field of view of 23 cm^2. An a-SE film, about 1000 μm thick, is used as an x-ray converter.

Dose Measurements

For 2D DSA, we set 2 programmable imaging modes with the FPD system: standard-dose mode and low-dose mode, each of which has different dose rate and image processing characteristics. The conventional-dose mode of I.I.-TV system used was a routine one for cerebral angiography at our institution. We compared the radiation dose

Table 1: Technical features of FPD system and I.I.-TV system

Feature	FPD system	I.I.-TV system
Total filtration	3 mm of Al + 0.3 mm of Cu	3 mm of Al
Additional filtration	None	None
Frame rate		
Cine mode	30 fps	30 fps
Fluoroscopy mode	15 fps	15 fps
Image matrix format	1440 × 1440	1024 × 1024
Field of view	9 inches	12 inches

Note:—FPD indicates flat panel detector; I.I.-TV, image intensifier television; fps, frames per second.

delivered to a 15-cm-thick block phantom (MIX-DP phantom; Sangyo Kagaku, Okayama, Japan) using 3 dose modes (standard-dose mode of FPD system, low-dose mode of FPD system, and conventional mode of I.I.-TV system). Each dose mode was obtained with the following exposure setting: low-dose mode of FPD system, 69 kVp, 14.1 mAs, and a 13:1 antiscatter grid with 1.0 m source-to-image distance (SID); standard-dose mode of FPD system, 69 kVp, 28.3 mAs, 13:1 antiscatter grid with 1.0 m SID; and conventional-mode of I.I.-TV system, 70 kVp, 14.9mAs, 10:1 antiscatter grid with 0.95 m SID. DSA was performed in an identical manner, using the same positioning and technique and an experienced investigator (N.Od.), delivering the radiation to the phantom to simulate a complete angiographic procedure. The exposures generated in any configuration or mode were measured using a model 9015 dosimeter with a 6-mL ion chamber (Radcal Corporation, Monrovia, Calif). For this study, the relative positions of the radiographic tube, procedure table, and detector (FPD or I.I.-TV) were fixed for both systems. The distances from the source tube to the table surface, from the table surface to the detector, and between the tube and the image detector were 80, 20, and 100 cm, respectively. For each measurement, the dosimeter was centered in the direct path of the beam and under the phantom (ie, at the table surface). The measured radiation exposure rate thus corresponded to the skin entry dose that would have been experienced by the average patient under identical imaging conditions.

Phantom Design and Subject Selection

An anthropomorphic vascular phantom (Renaissance of Technology, Shizuoka, Japan) consisted of a 19-cm-diameter cylinder made of silicone rubber designed to simulate the bilateral intracranial arteries with various intracranial aneurysms. Two types of simulated aneurysms (17 aneurysms with diameter of 3 mm and 15 aneurysms with diameter of 6 mm) were placed on the simulated internal carotid artery, anterior cerebral artery, and middle cerebral artery (Fig 1). Of all 32 aneurysms, 15 had a bleb with diameter of 2 mm, which was mounted at a tip onto the surface of the aneurysm. For both systems, 2D DSA was obtained from 2 series consisting of the subtraction mask images and the opacified images, all of which are engineered to the same specifications and capabilities as the DSA techniques used in our dose measurement studies. For opacified image, we sank the vascular phantom into a column-shaped container filled with 3 kinds of contrast material concentration (300, 150, and 100 mg I/mL) so as to fill the cylinder tubes of the phantom with the contrast material without introduction of air bubble. For each of 3 concentrations of contrast material, we obtained 2D DSA using the following 3 DSA techniques in 4 directions (posteroanterior, left or right posterior oblique, lateral, and craniocaudal): the standard-dose mode of FPD system, the low-dose mode of FPD system, and the conventional-dose mode of I.I.-TV system. Thus, a total of 72 cerebral angiograms (4 directions × bilateral internal carotid arteries × 3 DSA modes × 3 kinds of contrast material concentration) were prepared in this study. A fellowship-trained neuroradiologist (Y.H.) interpreted these angiographies and selected the 57 simulated aneurysms (with bleb, 20; without bleb, 37) for each contrast material concentration and angiographic mode based on sufficient visualization of the simulated aneurysms and blebs at optimum angle. Therefore, the aneurysms and blebs, which were insufficiently visualized because of overlapping structures, were excluded for the subjective evaluation and observer performance study.

Subjective Evaluation of 2D DSA

First, 2 neuroradiologists (S.K, N.Oh.) independently evaluated the image quality of the 2D DSA regarding the depiction of simulated aneurysms at separate session. These radiologists subjectively rated the depiction of simulated aneurysms using a 5-point scale: 5 (aneurysm was clearly visualized), 4 (good), 3 (reasonably good), 2 (poor), and 1 (very poor). After independent interpretations were performed, the differences in assessment of both observers were resolved by consensus.

Observer Performance Study

We next performed an observer performance study. Seven radiologists, including 4 board-certified interventional radiologists and 3 radiology residents with 4 years of experience in performing cerebral angiography, participated as observers. Before the test, the observers were informed that 1) the purpose of this study was to evaluate the radiologists' performance in detecting simulated aneurysmal blebs, 2) this study included simulated aneurysms with and without blebs, and 3) a simulated aneurysmal bleb was 2 mm in diameter (no more than 1 bleb per aneurysm). The number of aneurysms with blebs was blinded to the observers in this study.

A total of 72 cerebral angiograms were prepared in order at 9 reading sessions (3 dose modes × 3 contrast material concentrations). For each observer, in each readout session, the 8 angiograms (4 projections with 1 dose mode per each carotid artery) were randomized by computer. For each aneurysm, the readers were asked to state the presence or absence of an aneurysmal bleb and to rank their level of confidence on a 5-point scale, as follows 1, definitely present; 2, probably present; 3, uncertain; 4, probably not present; and 5, definitely not present. To avoid learning-curve effects, the time interval between reading sessions was at least 1 week.

Display of Images

For both FPD and I.I.-TV, each 2D DSA was displayed and interpreted on a high-resolution 1560 × 2048 (Barco, Kortrijk, Belgium) monitor. The observers were permitted to manipulate the monitor brightness and contrast with a track ball or push buttons. For both systems, DSA images were postprocessed with noise reduction using recursive filter and edge enhancement.

Statistical Analysis

For subjective evaluation, statistical analyses were performed with a statistical software package (StatView 5.0; SAS Institute, Cary, NC). For the scores of image quality, all results were expressed as the mean ± SEM for each contrast material concentration and dose mode. A Wilcoxon signed rank test was performed on the results to assess the statistical significance of the different scores assigned to the I.I. and FPD images. A P value of less than 0.05 was considered to indicate a statistically significant difference. To evaluate the level of

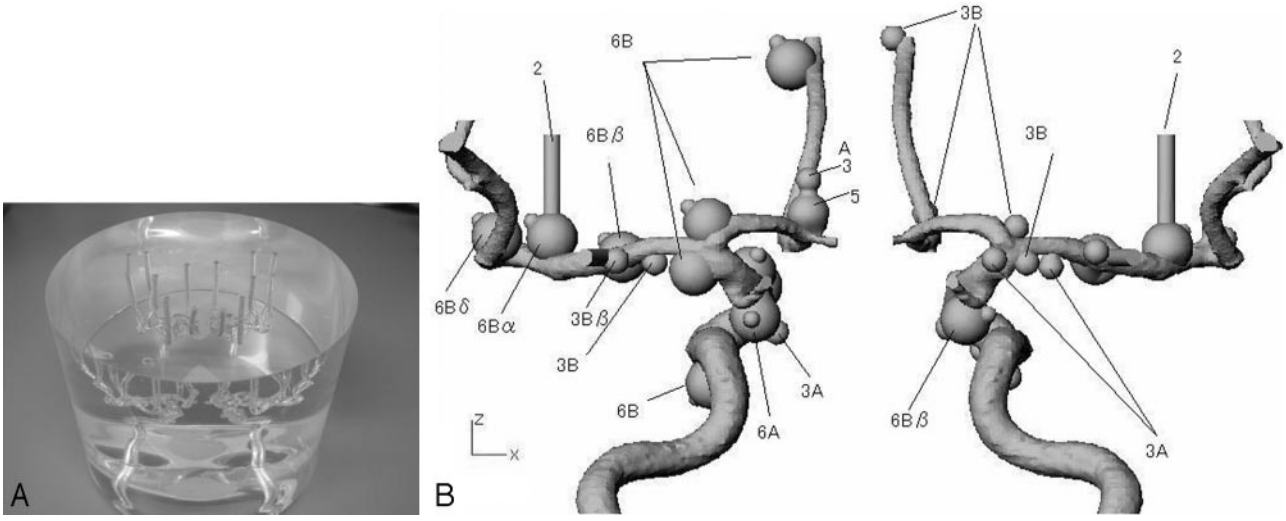

Fig 1. Photograph (*A*) and schematic drawing (*B*) of the anthropomorphic vascular phantom used in this study. The phantom was designed to simulate the intracranial arteries with a total of 32 aneurysms. Of 32 aneurysms, 15 had a bleb with diameter of 2 mm.

Table 2: Subjective evaluation for the 2D DSA regarding the depiction of simulated aneurysms

Contrast Material Concentration & Dose Mode	Score for Image Quality						
	5	4	3	2	1	Mean ± SD*	*P*
300 mgI/mL							
Standard-dose mode of FPD system	57	0	0	0	0	5.00 ± 0.00**	.038
Low-dose mode of FPD system	57	0	0	0	0	5.00 ± 0.00**	.038
Conventional-dose mode of I.I.-TV system	52	3	2	0	0	4.88 ± 0.43	
150 mgI/mL							
Standard-dose mode of FPD system	55	1	1	0	0	4.95 ± 0.29**	<.001
Low-dose mode of FPD system	52	4	1	0	0	4.90 ± 0.36**	<.001
Conventional-dose mode of I.I.-TV system	41	10	5	1	0	4.60 ± 0.73	
100 mgI/mL							
Standard-dose mode of FPD system	41	12	4	0	0	4.65 ± 0.61**	<.001
Low-dose mode of FPD system	39	13	5	0	0	4.60 ± 0.65**	<.001
Conventional-dose mode of I.I.-TV system	1	15	26	13	2	3.00 ± 0.85	

Note:—DSA indicates digital subtraction angiography; FPD, flat panel detector; I.I.-TV, image intensifier television. Data are mean ± SD of scores for image quality evaluated using a 5-point scale (1, clearly visualized; 2, good; 3, reasonably good; 4, poor; 5, very poor)
** Significantly higher to I.I.-TV system (the Wilcoxon signed rank test).

interobserver agreement of scores of image quality, a Kendall *W* test was performed on the independent scores from 2 radiologists before the consensus review. Kendall *W* coefficients between 0.5 and 0.8 were considered to indicate good agreement and coefficients higher than 0.8 were considered to indicate excellent agreement.

For the observer performance study, the resultant 3591 observations (57 aneurysms per 3 kinds of contrast material concentration, 3 dose modes, and 7 readers) were calculated separately each on 2 bases (per contrast material concentration and per dose mode) and analyzed according to receiver operating characteristic (ROC) analysis. Estimates of the area under the ROC curve and SDs were computed using the computer program (LABROC5) provided by Metz et al.[11] Observer performance was expressed in mean areas under the ROC curve (Az). The 95% confidence intervals (CI) for the differences in areas under the ROC curve among the various imaging modalities provided evidence of whether the difference was significant. The statistical significance of the differences in observer performance (Az) among 3 DSA modes was estimated by use of the paired Student *t* test. A P value $< .05$ was considered to indicate a statistically significant difference.

Results

Dose Measurements

A 2D DSA with I.I.-TV system and both dose modes with FPD system consisted of 4 frames as mask and 14 frames as injection run. The mean dose measurements with a phantom during 2D DSA were 0.36 mGy/frame with the low-dose mode of FPD system, 0.72 mGy/frame with the standard-dose mode of FPD system, and 0.76 mGy/frame with the I.I.-TV system. Thus, the 2D DSA in dose measurements with low-dose mode of FPD system showed dose reductions of 50.0% (from 0.72 mGy/frame to 0.36 mGy/frame) compared with standard-dose mode of FPD system and 52.6% (from 0.76 mGy/frame to 0.36 mGy/frame) compared with I.I.-TV system.

Subjective Evaluation

With regard to the depiction of aneurysms on 2D DSA among the 3 dose modes, the results of the final consensus reviewed by 2 radiologists are summarized in Table 2. There was no significant difference between the low-dose mode and standard-dose mode

Table 3: Diagnostic performance according of each observer regarding the detection of the simulated aneurysmal blebs

Contrast Material Concentration & Dose Mode	Observer							Mean Az
	1	2	3	4	5	6	7	
300 mgI/mL								
Standard-dose mode of FPD system	0.93	0.91	0.89	0.92	0.91	0.92	0.94	0.92
Low-dose mode of FPD system	0.89	0.89	0.91	0.92	0.92	0.94	0.95	0.92
Conventional-dose mode of I.I.-TV system	0.92	0.91	0.86	0.98	0.87	0.95	0.90	0.91
150 mgI/mL								
Standard-dose mode of FPD system	0.81	0.79	0.83	0.83	0.83	0.80	0.82	0.82
Low-dose mode of FPD system	0.83	0.79	0.85	0.82	0.83	0.85	0.84	0.83
Conventional-dose mode of I.I.-TV system	0.80	0.78	0.85	0.81	0.82	0.84	0.82	0.82
100 mgI/mL								
Standard-dose mode of FPD system	0.84	0.88	0.87	0.80	0.93	0.87	0.80	0.86*
Low-dose mode of FPD system	0.84	0.88	0.86	0.79	0.93	0.87	0.79	0.85*
Conventional-dose mode of I.I.-TV system	0.67	0.55	0.54	0.57	0.55	0.54	0.52	0.56

Note:—Az indicates areas under the receiver operating characteristic curve; FPD, flat panel detector; I.I.-TV, image intensifier television.
* Significantly higher to I.I.-TV system ($P < .01$).

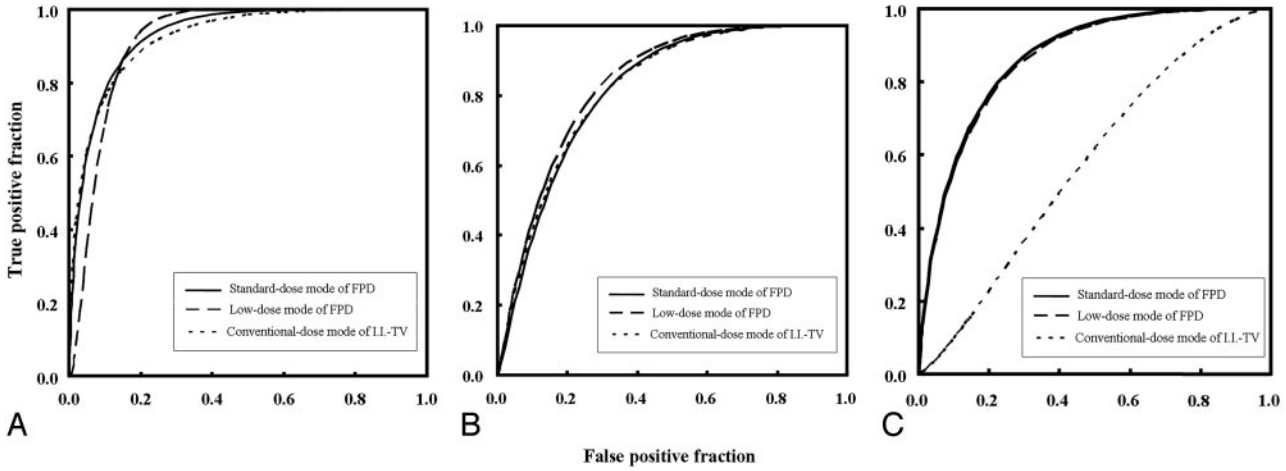

Fig 2. ROC curves for the detection of simulated aneurysmal blebs with 3 different contrast material concentrations: 300 mg I/mL (*A*), 150 mg I/mL (*B*), and 100 mg I/mL (*C*). For each contrast material concentration, graph shows the 3 composite ROC curves generated from the pooled data of the 7 observers' results with the standard- (*solid line*) and low-dose modes of FPD (*dashed line*) and the conventional-dose mode of I.I.-TV (*dotted line*) systems.

of FPD system with any kind of contrast material concentration. The depiction of aneurysms with both dose modes of FPD system was significantly superior to the I.I.-TV system with any kind of contrast material concentration. In particular, the difference was most prominent at a concentration of 100 mg I/mL (4.60 ± 0.65 versus 3.00 ± 0.85, $P < .05$).

For subjective evaluation of 2D DSA, interobserver agreement between the 2 radiologists in rating the depiction of aneurysms was good or excellent for the standard- and low-dose modes of the FPD system and the conventional-dose mode of the I.I.-TV system, respectively, with Kendall *W* values (τ) of 1.00, 1.00, and 0.83 for rating of 2D DSA with 300 mg I/mL, 0.89, 0.88, and 0.73 for rating of 2D DSA with 150 mg I/mL, and 0.77, 0.68, and 0.60 for rating of 2D DSA with 100 mg I/mL.

Observer Performance Study

Table 3 and Fig 2 show the mean areas under the ROC curve (Az) for each mode. With concentrations of 300 and 150 mg I/mL, the mean Az values for images obtained with the low-dose mode of FPD (mean Az value = 0.92 and 0.83) in the detection of blebs were not significantly different from those obtained with the conventional dose mode of I.I.-TV (mean Az value = 0.91 and 0.82), respectively (Fig 3). In contrast, the mean Az value at 100 mg I/mL was significantly better for low-dose mode of FPD than for conventional-dose mode of I.I.-TV (mean Az value, 0.85 versus 0.56; $P < .01$) (Fig 4). For any contrast material concentration, there were no significant differences in the mean Az values between the standard- and low-dose modes of the FPD system.

Discussion

Our subjective evaluation for the depiction of simulated aneurysms on the 2D DSA demonstrated that the FPD system at half the exposure dose of the I.I.-TV system was significantly superior to the I.I.-TV system with any kind of contrast material concentration. Our observer performance study showed that the low-dose mode of FPD system allowed equivalent or superior detectability of the simulated blebs compared with the conventional-dose mode of the I.I.-TV system. This combined subjective and observer performance studies demonstrated that, with a radiation dose reduction of 50%, the diagnostic performance of the FPD system is still superior to that of the I.I.-TV system.

The good performance of the direct conversion type FPD system seems to be a result of a combination of spatial resolution and signal-to-noise ratio expressed as the detective quantum efficiency (DQE). Modulation transfer function (MTF) is generally accepted as the most important parameter of spatial

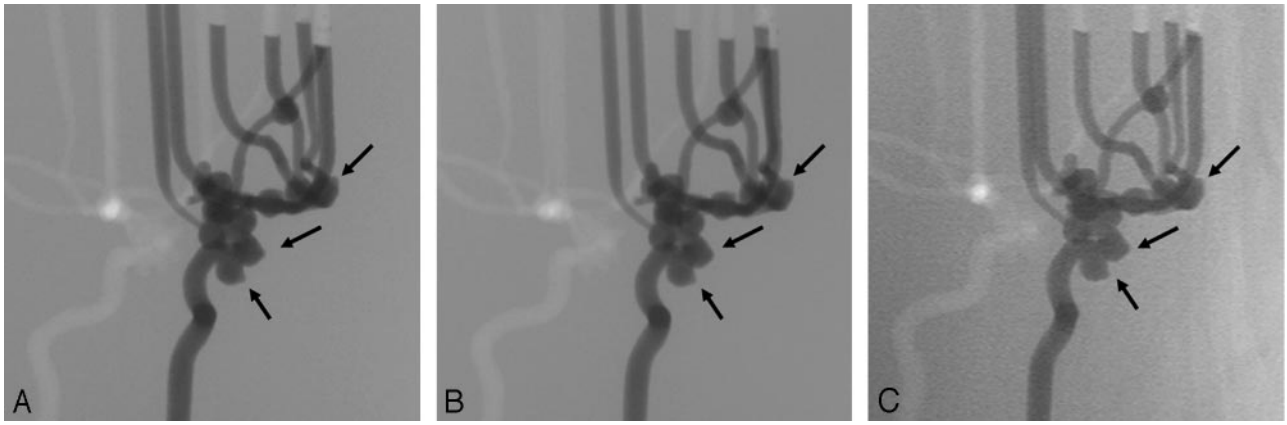

Fig 3. 2D DSA from the left anterior oblique view at 300 mg I/mL obtained with standard-dose mode of FPD system (*A*), with low-dose mode of FPD system (*B*), and with conventional-dose mode of I.I.-TV system shows blebs (*arrows*) (*C*). For the depiction of aneurysmal blebs, there is no particular difference among the 3 dose modes.

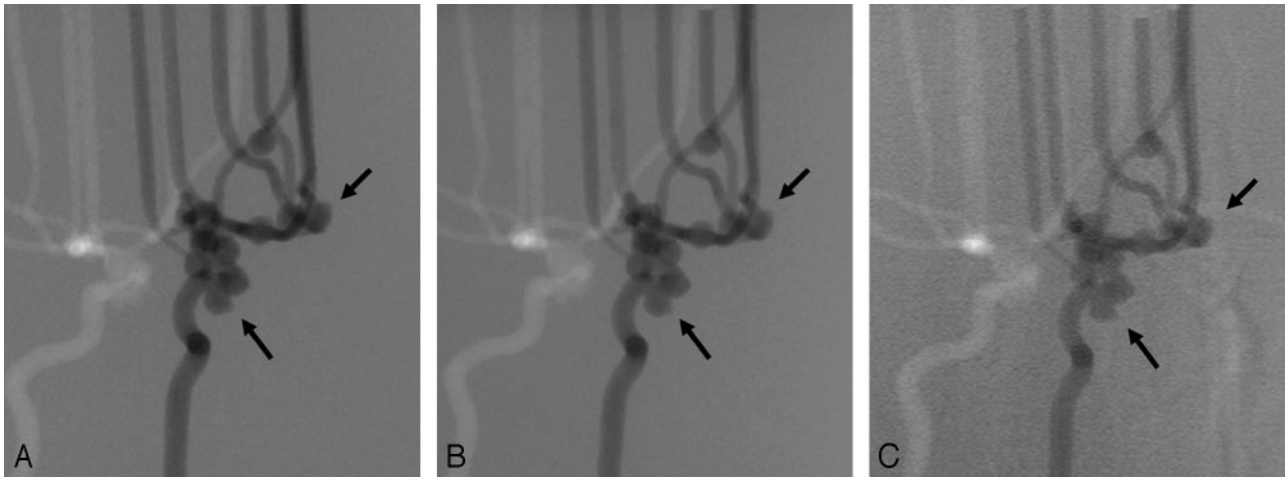

Fig 4. 2D DSA from the left anterior oblique view at 100 mg I/mL obtained with standard-dose mode of FPD (*A*), with low-dose mode of FPD (*B*), and with conventional-dose mode of I.I.-TV system shows blebs (*arrows*) (*C*). For the depiction of aneurysmal blebs, the images obtained with both dose modes of FPD system are superior to those obtained with the I.I.-TV system.

resolution for characterizing the performance of a detector system. Although measurements of physical imaging characteristics cannot be directly related to expected observer performance in a diagnostic setting, there is general agreement that a higher MTF is indicative of superior image quality. The FPD used in this study shows a high MTF in the previous theoretic analysis and experimental testing.[12,13] Voelk et al[14] and Strotzer et al[8] have reported that the FPD, due to its high DQE, has the potential for dose reduction while maintaining diagnostic accuracy. In the FPD of direct conversion type, absorbed x-ray photons are directly converted to electron hole pairs in a conversion layer (eg, amorphous selenium), and then collected as electric charges on storage capacitors.[15-17] Therefore, the capability of performing a simple conversion process with the FPD of direct conversion type reduces the scatter fraction of electrons and light photons within the detector in the underpenetrated regions of the image, and improves signal-to-noise ratio. In the ROC analysis of our study, the Az value for the detection of blebs was as low as 0.56 with I.I.-TV system at concentration of 100 mg I/mL. This result may be due to a low image contrast with I.I.-TV system, as well as the spatial resolution that results in the video system. Image blurring in I.I.-TV system can result from the scattering of x-ray beams, light, or both in the detector. Veiling glare, which has been a term to describe the scatter of electrons and light photons within an x-ray I.I.-TV, reduces image contrast.[18] Although we did not perform a systematic analysis, more prominent reduction of image contrast was noted with 2D DSA by using I.I.-TV system (Fig 4*C*).

One of the major advantages of the FPD is the wide dynamic range, which improves contrast throughout the image and allows better visualization of low-contrast regions.[19-21] The dynamic range of our FPD system is 1:10,000 according to the manufacturers' specifications. Although a wide dynamic range is the main feature of this FPD system, the diagnostic task in our phantom study mainly requires high contrast resolution and may be more limited by the signal-to-noise ratio and high spatial resolution rather than the wide dynamic range.

In observer performance study, we examined the diagnostic performance of both systems in the detection of the simulated aneurysmal blebs. Our study design was chosen for several reasons. Aneurysmal blebs represent clinically important lesions in patients with aneurysms, because the presence of an aneurysmal bleb may indicate a higher risk of bleeding from an unruptured internal carotid aneurysm.[22] In addition, detec-

tion of aneurysmal blebs could be chosen to acquire good discrimination of imaging qualities. The simulated aneurysms with diameter of 3 or 6 mm detected too easily would have resulted in a score of image quality too close to "definitely present," which would not have been useful in comparing imaging systems. We chose aneurysmal blebs, which were small objects placed at a tip onto the surface of the aneurysm, because spatial resolution and signal intensity-to-noise ratio with FPD can be expected to be an important contributing factor in the detectability of the blebs. The range of Az values in our observer performance study shows that depiction of the experimentally created aneurysmal blebs was appropriate for the evaluation of the imaging system and exposure level combinations.

There are several limitations in our study. First, we arbitrarily selected the range of contrast material concentration of contrast agent to achieve good discrimination of 3 dose modes, because these have not been evaluated in the previous literature. Therefore, the use of concentration of 100 mg I/mL may not reflect the clinical reality. However, it is important to note that FPD system at half the exposure dose of I.I.-TV system was not inferior to I.I.-TV system with any kind of contrast material concentration. Second, a limitation of our phantom design was that no superimposed bone skull structures were simulated. Therefore, this phantom, which has nothing to produce the x-ray attenuation or scatter of a skull, may have collected much more photons for generating these images than would have been the case in human angiography. In addition, the absorption of the phantom in our study was much more homogeneous than the absorption of different areas of the actual human head (eg, the areas superimposed over the skull base versus those superimposed over the brain only), and our phantom was much less dynamic in terms of absorption range than an actual human head. Because of these reasons, one might assume that the low dose mode of the FPD system (with a 50% dose saving) could not always be used during all the intervention and working with the FPD standard dose mode could be necessary. In this study, however, it seems impossible to know whether these factors with phantom design would tend to overestimate or underestimate the performance of FPD system. In fact, in our institution, the low-dose mode of the FPD has been routinely used for cerebral angiography for about 2 years without any clinical problems. We believe that it is important to compare 2 systems in the same experimental condition. Third, our phantom experiment found no significant difference in image quality between the standard- and low-dose modes of FPD. Therefore, the lowest possible dose for the given diagnostic task could not be determined. Fourth, we evaluated only radiation dose during 2D DSA. Both fluoroscopy and DSA contribute to radiation dose in patients undergoing interventional procedures, though previous reports have not mentioned the precise percentage of radiation dose delivered by each of the 2 methods during the course of an actual interventional procedure.[1,23-25] Therefore, the further investigation regarding the dose reduction of fluoroscopy with an angiography system by using the FPD is necessary.

In conclusion, our study should be regarded as a step toward appraising the use of FPD technology in interventional neuroradiology. Our results show that 2D DSA with FPD allows an equivalent or better diagnostic performance for evaluation of simulated aneurysmal blebs at half the conventional exposure dose used with I.I.-TV system. These results highlight the potential clinical advantages of the SE-based FPD, which offer the possibility of reducing the patient dose with no loss of image quality. Further study is required to determine the lowest possible dose for the given diagnostic task by using FPD systems.

References

1. AM Norbash, D Busick, MP Marks. **Techniques for reducing interventional neuroradiologic skin dose: tube position rotation and supplemental beam filtration.** *AJNR Am J Neuroradiol* 1996;17:41–49
2. Huda W, Peters KR. **Radiation-induced temporary epilation after a neuroradiologically guided embolization procedure.** *Radiology* 1994;193:642–44
3. Kuwayama N, Takaku A, Endo S, et al. **Radiation exposure in endovascular surgery of the head and neck.** *AJNR Am J Neuroradiol* 1994;15:1801–08
4. Merriam GR Jr, Focht EF. **A clinical study of radiation cataracts and the relationship to dose.** *Am J Roentgenol Radium Ther Nucl Med* 1957;77:759–85
5. Merriam GR Jr. **A clinical study of radiation cataracts.** *Trans Am Acad Ophthalmol Otolaryngol* 1956;54:611–53
6. Strotzer M, Volk M, Wild T, et al. **Simulated bone erosions in a hand phantom: detection with conventional screen-film technology versus cesium iodide-amorphous silicon flat-panel detector.** *Radiology* 2000;215:512–15
7. Ludwig K, Lenzen H, Kamm KF, et al. **Performance of a flat-panel detector in detecting artificial bone lesions: comparison with conventional screen-film and storage-phosphor radiography.** *Radiology* 2002;222:453–59
8. Strotzer M, Gmeinwieser J, Volk M, et al. **Clinical application of a flat-panel x-ray detector based on amorphous silicon technology: image quality and potential for radiation dose reduction in skeletal radiography.** *AJR Am J Roentgenol* 1998;171:23–27
9. Garmer M, Hennigs SP, Jager HJ, et al. **Digital radiography versus conventional radiography in chest imaging: diagnostic performance of a large-area silicon flat-panel detector in a clinical CT-controlled study.** *AJR Am J Roentgenol* 2000;174:75–80
10. Link TM, Rummeny EJ, Lenzen H, et al. **Artificial bone erosions: detection with magnification radiography versus conventional high-resolution radiography.** *Radiology* 1994;192:861–64
11. Metz CE, Herman BA, Shen JH. **Maximum-likelihood estimation of receiver operating (ROC) characteristic curves from continuously-distributed data.** *Stat Med* 1998;17:1033–53
12. Adachi S, Hori N, Sato K, et al. **Experimental evaluation of a-Se and CdTe flat-panel x-ray detectors for digital radiography and fluoroscopy.** *Proc SPIE* 2000;3977:38–47
13. Samei E, Flynn MJ. **An experimental comparison of detector performance for direct and indirect digital radiography systems.** *Med Phys* 2003;30:608–22
14. Voelk M, Strotzer M, Gmeinwieser J, et al. **Flat-panel x-ray detector using amorphous silicon technology: reduced radiation dose for the detection of foreign bodies.** *Investig Radiol* 1997;32:373–77
15. Rowlands JA, Hunter DM, Araj N. **X-ray imaging using amorphous selenium: a photoinduced discharge readout method for digital mammography.** *Med Phys* 1991;18:421–31
16. Chotas HG, Dobbins JT, Rabin CE. **Principles of digital radiography with large-area, electronically readable detectors: a review of the basics.** *Radiology* 1999;210:595–99
17. Zhao W, Ji WG, Debrie A, et al. **Imaging performance of amorphous selenium based flat-panel detectors for digital mammography: characterization of a small area prototype detector.** *Med Phys* 2003;30:254–63
18. Seibert JA, Nalcioglu O, Roeck WW. **Characterization of the veiling glare PSF in x-ray image intensified fluoroscopy.** *Med Phys* 1984;11:172–79
19. Aufrichtig R. **Comparison of low contrast detectability between a digital amorphous silicon and a screen-film based imaging system for thoracic radiography.** *Med Phys* 1999;26:1349–58
20. Spahn M, Strotzer M, Volk M, et al. **Digital radiography with a large-area, amorphous-silicon, flat-panel x-ray detector system.** *Investig Radiol* 2000;35:260–66
21. Floyd CE, Warp RJ, Dobbins JT, et al. **Imaging characteristics of an amorphous silicon flat-panel detector for digital chest radiography.** *Radiology* 2001;218:683–88
22. Beck J, Rohde S, el Beltagy M, et al. **Difference in configuration of ruptured and unruptured intracranial aneurysms determined by biplanar digital subtraction angiography.** *Acta Neurochir (Wien)* 2003;145:861–65
23. Balter S, Schueler BA, Miller DL, et al. **Radiation doses in interventional radiology procedures: the RAD-IR Study. Part III: Dosimetric performance of the interventional fluoroscopy units.** *J Vasc Interv Radiol* 2004;15:919–26
24. Miller DL, Balter S, Cole PE, et al. **Radiation doses in interventional radiology procedures: the RAD-IR study: part II: skin dose.** *J Vasc Interv Radiol* 2003;14:977–90
25. Miller DL, Balter S, Cole PE, et al. **Radiation doses in interventional radiology procedures: the RAD-IR study: part I: overall measures of dose.** *J Vasc Interv Radiol* 2003;14:711–27